

出國報告（出國類別：其他：國際會議）

赴紐西蘭參加地震工程研討會及參訪奧克蘭大學

服務機關：國立雲林科技大學

姓名職稱：李宏仁 營建技術服務暨材料檢測中心 主任

派赴國家：紐西蘭

出國期間：106年4月25日至106年5月2日

報告日期：106年5月4日

摘要

紐西蘭地震工程學會每年舉辦一次地震工程研討會，2017 年 4 月 27-29 日三天研討會在紐西蘭首都威靈頓舉行，大會共邀請三位國外主題講人(Keynote speaker)，另邀請發表論文講者計 28 位，加上投稿之論文口頭發表 109 篇、海報發表 76 篇，總計超過 200 篇研討會論文，是環太平洋地震帶著名的研討盛會。與會者除紐西蘭本地學者及工程師之外，還有來自澳洲、日本、美國、義大利、中國、韓國、台灣等地震帶國家的學者，世界一流地震工程學者專家聚集於此，本次赴會除汲取主辦單位辦理研討會之經驗，蒐集各國最新研究動態，回饋我方相關技術研發應有幫助。

筆者此行抵達威靈頓參加三天的研討會，協同博士生共發表 2 篇論文。三天研討會期間有兩晚晚宴交流，藉此社交活動認識與會者建立聯繫，並拓展我方研究之能見度。研討會過程筆者發現紐西蘭在地震工程領域之研究構想、技術其實非常先進，或是說想法具有前瞻開創性，但是因為紐西蘭地廣人稀，人口密度低且工業規模較小，許多建築仍為木構造，該國學者有許多創新之構想及研究專利，卻未必能有大量應用之機會。回顧歷史，許多地震工程領域創新之想法皆由紐西蘭學者發明，但是具體的工程應用，反而在美日等大國實現。所以開發創新與落實應用之間的落差，與國情及產業特性習習相關，地震工程之研究者也需要思考其研究如何應用於實務。

會後筆者專程前往奧克蘭大學拜訪其土木與環境工程學系教授 Ken Elwood，他也是該校地震工程研究中心主任(Director of the newest Centre of Research Excellence (CoRE), QuakeCoRE: Centre for Earthquake Resilience)，除參觀該校教學研究設施之外，我們也討論雙邊合作研究之可能課題，未來可配合運用我國國家實驗研究院國家地震工程研究中心第二實驗設施新建之高速振動台(地震模擬器)，共同研究老舊鋼筋混凝土構架之崩塌行為，此行已邀請 Ken Elwood 教授於 8 月訪台期間再進一步磋商具體合作內容及振動台實驗設計細節，為此行另一收穫。

目次

一、目的.....	1
二、過程.....	1
三、心得.....	2
四、建議事項.....	3
五、(附錄).....	4

一、目的

此行參加在紐西蘭首都威靈頓舉行的紐西蘭地震工程研討會目的有三，一為發表會議論文兩篇，展現我們近期的研究成果，提升我國相關研究之國際能見度；二為蒐集其他環太平洋地震帶國家的最新研究近況發展，作為我方後續研究規劃之參考；三為觀摩紐西蘭地震工程學會如何成功地辦理此一研討會，竟然能吸引如此多的國際學者與會，大會場地安排、設施設備、手冊編排、活動流程及時間管理等，皆有可學習之處，可作為我方日後辦理國內外學術研討會之參考。

奧克蘭大學為紐西蘭最高學府，常年位居世界大學百大排名之內，其研究成果佔紐西蘭七成以上，足見其重要性。此行於研討會後順道前往奧克蘭大學土木與環境工程學系拜會 Ken Elwood 教授，他也是該校地震工程研究中心主任(Director of the newest Centre of Research Excellence (CoRE), QuakeCoRE: Centre for Earthquake Resilience)，過去他曾經訪問台灣，對於台灣地震工程研究有一定程度之了解，此行除參觀該校教學研究設施之外，我們也討論雙邊合作研究之可能課題，未來可配合運用我國國家實驗研究院國家地震工程研究中心第二實驗設施新建之高速振動台(地震模擬器)，雙邊共同研究老舊鋼筋混凝土構架之崩塌行為。

二、過程

此行 4 月 25 日凌晨自桃園國際機場起飛，經澳洲轉機至奧克蘭機場已是當地時間下午 6 點半，過夜後 26 日由紐西蘭友人方接待移動到南方 630 公里遠的威靈頓市準備隔天的研討會，27、28 日共發表我方兩篇論文，27-29 日間共參加六個論文報告時段，聆聽三場專題演講，參加兩場社交晚宴。30 日由紐西蘭友人方接待移動回到奧克蘭市區拜會 Ken Elwood 教授深談研究規劃及未來合作方向，5 月 1 日上午參觀奧克蘭大學後搭機返台。過程照片如圖 1 至圖 8，主要活動細節如下：

4/27 星期四 紐西蘭地震工程研討會 NZSEE 2017 研討會第一日

下午聆聽至參加紐西蘭 2016 Kaikoura Earthquake (Mw =7.8)的特別時段，聆聽紐西蘭官方及專家學者對於該地震特性及震害之檢討，蒐集多篇具有參考價值之文章內容，其危樓勘災經驗及震後安全評估方法，也可以作為台灣在美濃地震後行政院推動之「都市危險及老舊建築物加速重建獎勵條例」建築物性能評估作業之參考。

下午筆者發表第一篇論文(詳附件 1)並於論文口頭報告時段蒐集資料，並聆聽第一位主題講者 Rene Lagos 教授之演講，講述智利最新的鋼筋混凝土建築耐震設計觀念，獲益良多。晚上參加在大廳舉辦歡迎酒會。

4/28 星期五 紐西蘭地震工程研討會 NZSEE 2017 研討會第二日

上午先聽第二位主題講者 Gianmario Benzoni 教授之演講，介紹全球隔震消能元件之最新發展，而後參加兩個論文口頭報告時段蒐集資料，並偕同本人指導之博士生陳錫慶先生發表第二篇論文(詳附件 2)。下午有一個特別時段是地震損壞控制之結構設計專題時段，晚上參加大會舉辦之研討會晚宴。

4/29 星期六 紐西蘭地震工程研討會 NZSEE 2017 研討會第三日

上午先聽第三位主題講者 Akira Wada 演講，講述日本大都市之耐震設計規劃，開拓視野。接著聆聽兩個論文發表時段，下午有一個降低震害及快速復原的特別時段，紐西蘭地震工程研究除了防災之外，也非常注重災後如何快速復原之研究。下午三點頒發研討會各個票選獎項。

4/30 星期日 洽談台紐雙邊合作研究

移動回到奧克蘭市區，拜會奧克蘭大學土木與環境工程系 Ken Elwood 教授，深談研究規劃及未來合作方向，討論雙邊合作研究之可能課題，未來可配合運用我國國家實驗研究院國家地震工程研究中心第二實驗設施新建之高速振動台(地震模擬器)，雙邊共同研究老舊鋼筋混凝土構架之崩塌行為，Ken Elwood 教授將負責柱承載能力之研究規劃，預定指派一位博士後研究員來台負責振動台實驗，筆者將專注於近斷層地震下鋼筋混凝土構架接頭破壞與倒塌行為研究，未來可促成台紐雙邊科技部跨國合作研究計畫。

5/1 星期一 參觀奧克蘭大學

上午參觀奧克蘭大學，觀摩該校教學研究設施，作為本校相關建設之參考。下午啟程搭機返台

三、心得

筆者參加紐西蘭地震工程研討會，強烈感受到紐西蘭官方及工程師對於地震災害、建築結構安全、震後使用性能之關切，與會的國內外專家學者發表之研究論文品質很高，有許多領先潮流、具獨創性之抗震技術，猶如服裝時尚展在巴黎，紐西蘭地震工程研討會算是地震工程研究之時尚展也不為過，到此一覽世界最新研究趨勢，深受啟發。

此行觀摩紐方辦理研討會之規劃，包括場地安排、設施設備、議程活動、時間控管、乃至於食物及晚宴之安排，都在水準以上，筆者最深刻印象就是上台簡報的設備，是類似選舉演講或辯論的布設，除了大投影幕，地面有電視及倒數計時之時間，讓講者可以面對聽眾且注意時間，時間到主控台直接切斷投影片撥放，時間控制超級嚴格，確保研討會流暢。這些都是我方未來舉辦類似研討會可以參考改進之處。

此行最後拜會奧克蘭大學土木與環境工程系 Ken Elwood 教授，了解紐方研究近況並促成未來可能之雙邊研究計畫，是此行之意外收穫。參觀奧克蘭大學發現，其實紐西蘭校方對於經費之使用、設備之投資及使用管控非常嚴格，是一個非常重視目標及資源有效分配及利用的國家，相對於台灣時常誤將手段當作目的，造成科研單位資源錯置及浪費，我國人口及國力絕對在紐西蘭之上，但地震工程研究能量及成就卻似乎不如紐西蘭來得亮眼，確實值得我方省思。

四、建議事項

- 1.建議應盡可能爭取經費補助學人持續參加紐西蘭地震工程研討會，此研討會匯集世界一流學者及論文報告，可供蒐集之資料及經驗豐富，有助於提升我方之研究視野。
- 2.本次會議期間發現紐西蘭的留學生有許多是中國學生，也有許多在中國大陸唸博士班的學生出國參加研討會並上台發表論文，台灣方面多數是教授及博士後研究員上台報告，僅少數由博士生上台，建議我國政府應多多鼓勵台灣博碩士生出國參加國際研討會，從寬補助國內學人出席相關專業技術交流會議，除了提升我國研究能見度，亦有助於我國學生之國際觀跟膽識。
- 3.紐西蘭地震工程學會每年舉辦地震工程研討會，經驗豐富，會場各項軟硬體安排可以作為我方舉辦類似研討會之參考。
- 4.我國國家地震工程研究中心之編制、設備及規模均遠遠超過紐西蘭奧克蘭大學，雖然我國之地震工程研究成果豐碩，但是紐方地震工程國際能見度並不亞於我方，國際研討會之舉辦能力及頻率也是很大的差異，紐西蘭地震工程學會能每年舉辦國際研討會，其募款能力及邀請國際講者的人脈，是我方需要好好學習之處。

五、(附錄)



圖 1 註冊



圖 2 會場展示廳



圖 3 論文簡報

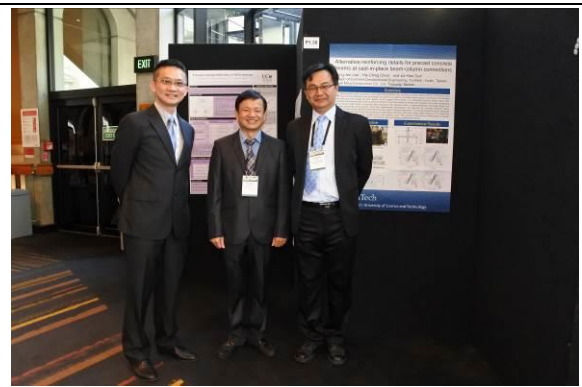


圖 4 與台灣學者合影



圖 5 論文簡報

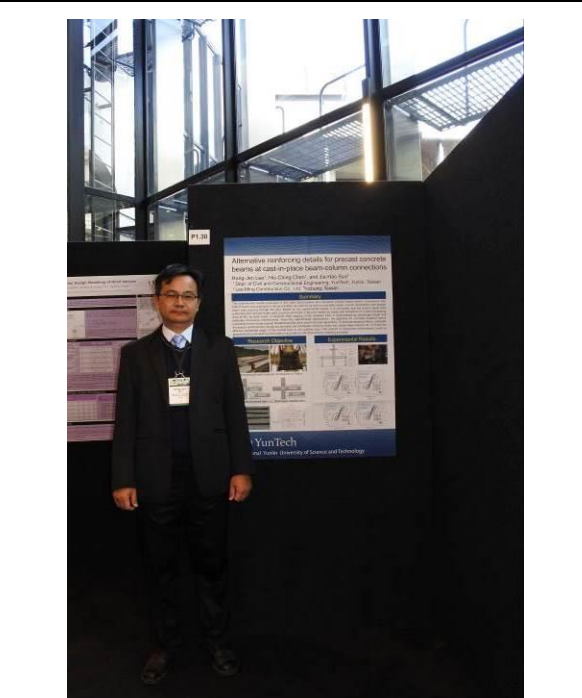


圖 6 論文海報合影



圖 7 歡迎晚宴

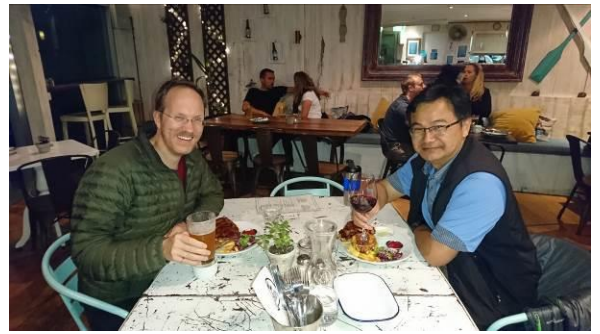


圖 8 與 Ken Elwood 餐敘

Alternative reinforcing details for precast concrete beams at cast-in-place beam-column connections

H.J. Lee & H.C. Chen

Department of Civil and Construction Engineering, National Yunlin University of Science and Technology, Yunlin, Taiwan.

J.H. Syu

Lee Ming Construction Co. Ltd, Taichung, Taiwan.



2017 NZSEE
Conference

ABSTRACT: The paper presents an experimental investigation on alternative reinforcing details for bottom bars of precast concrete beams at cast-in-place beam-column joints to achieve behaviour as for monolithic reinforced concrete beam-column connections. To relief steel congestion and fabrication difficulty, it is proposed to use head bars for bottom bars protruded from precast beams and anchored in the middle of the beam-column joint. Six interior beam-column connection specimens were tested under reversed cyclic loading. The primary test variables were the anchorage of bottom beam bars in the joint and the presentence of transverse beams. Within the experimental programme, four connection specimens with bottom beam bars anchored in the middle of the joint performed as good as the other two benchmark specimens with continuous beam bars. Hysteretic behaviour, including strength degradation, stiffness degradation, and energy dissipation, were evaluated in accordance with acceptance criteria for special moment-resisting frames. On the basis of experimental results, design recommendations are drawn for such emulative precast beam-column connections.

1 INTRODUCTION

Many possible arrangements of precast concrete members and cast-in-place concrete forming ductile moment-resisting frames have been used in many countries (Park, 2002; Pampanin, 2005; Watanabe, 2007). Figure 1 shows the most commonly used arrangement of emulative precast beam-column connections in Taiwan. Precast beam elements are placed on the edges of bottom precast columns, and then the reinforcement is placed in the beam-column joint core, the top of the beams, and the slabs. Afterward, the cast-in-place concrete is placed to form an emulating monolithic reinforced concrete beam-column-slab connection.

This arrangement of precast elements leads to a large reduction on site formwork and labours, but also arise a difficulty of steel congestion within the cast-in-place joint, where the bottom beam bars, protruding from the precast beam elements, need to be extended to the far face of joint core and bent up for anchorage. Hence the bottom beam bars framing from two opposite faces of a joint have to be well staggered in order not to overlap each other. Even so, the bent-up hook extensions of bottom beam bars may conflict with the inner ties within the joint core. Due to steel congestion, the quality of cast-in-place concrete in the joint core may be questioned.

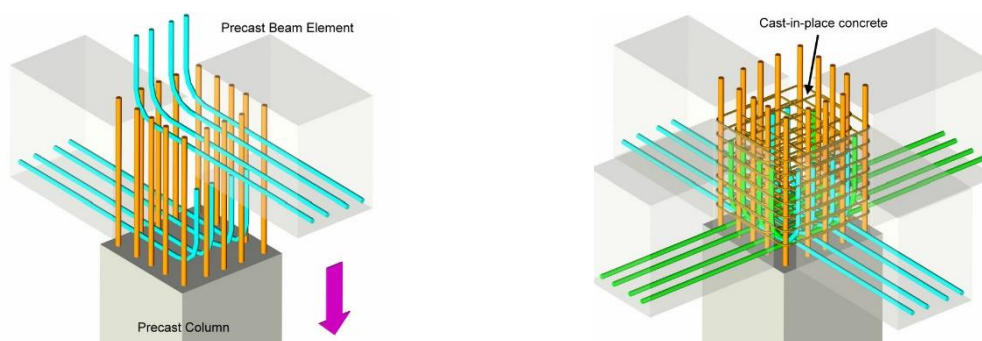


Figure 1. Conventional arrangement for connecting precast beams at a cast-in-place joint.

The use of headed reinforcement provides a promising way to ease the steel congestion in a beam-column joint (Wallace et al., 1998; Kang et al., 2009). This paper proposes alternative reinforcing details to terminate bottom beam bars at the joint middle with anchored plates or heads, provided that the headed bars have adequate anchorage length and confined with closely-spaced joint hoops and ties. The proposed alternative reinforcing details of bottom beam bars could liberate the difficulties in the design, erection, and fabrication of the precast beam elements at cast-in-place beam-column joints, as shown in Figure 2. To verify this idea, an experimental programme was conducted to investigate the use of headed bottom beam bars terminated in the joint middle in comparison with the conventional design.

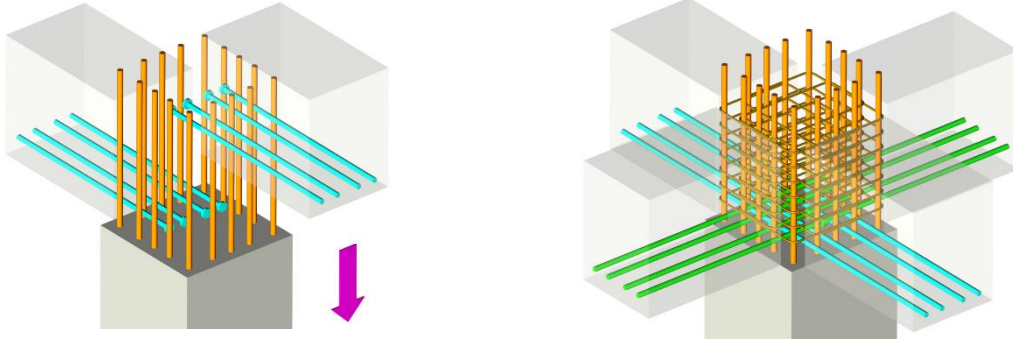


Figure 2. Proposed alternative reinforcing details for connecting precast beams at a cast-in-place joint.

2 TEST PROGRAMME

2.1 Connection design

Six emulative precast beam-column connections were tested under reversed cyclic loading. Figure 3 shows the matrix of test specimens. Three joint specimens, designated as Group A, used eight and four D25 reinforcing bars for the longitudinal reinforcement in the beam top and bottom, respectively, resulting in an unequal reinforcement ratio in the beam section. The other three specimens, designated as Group B, used six D25 reinforcing bars symmetrically for the top or bottom beam reinforcement. The total amount of beam longitudinal reinforcement are 12 D25 reinforcing bars, and thus the design shear force of the joint (V_u), which is estimated by the method recommended by ACI 352R-02 (ACI-ASCE Committee 352, 2002), is approximately equal to 2720 kN for each test connection.

$$V_u = 1.25f_y(A_{s,top} + A_{s,bot}) - V_{col} \quad (1)$$

$$V_{col} = \frac{(M_{pr}^+ + M_{pr}^-) L_b}{(L_b - h_c) L_c} \quad (2)$$

where $A_{s,bot}$ is the area of bottom beam bars; $A_{s,top}$ is the area of top beam bars; f_y is the specified yield strength of reinforcement; V_{col} is the column shear force in equilibrium with the probable beam moments M_{pr} at the joint faces, which were determined using a bar stress of $1.25f_y$, for positive and negative bending moments, respectively; L_b is the unit beam length (4.5 m for tested specimens); L_c is the unit column length (3 m for tested specimens) or the equivalent story height; h_c is the column depth of 500 mm.

All test specimens had a square column section of 500x500 mm detailed with 12 D25 Grade 420 longitudinal reinforcing bars and D13 Grade 490 transverse hoops and ties at a spacing of 100 mm. The Grade 490 reinforcement was used to reduce the amount of transverse reinforcement for confinement of 55-MPa concrete column.

Table 1 shows the material properties and connection design parameters calculating using ACI 352R-02 method for each test specimen. The measured yield and ultimate strengths of flexural reinforcement are 470 MPa and 670 MPa, respectively. All specimens were designed to meet the requirements for special moment frames per ACI 318, except the alternative details of bottom beam bars, which are examined in this program. The design shear stress acting on the joint is controlled to be $1.67\sqrt{f'_c}$ MPa, which is specified value for interior joints confined on all four faces. In other words, the design joint shear for Specimen A3 or B3 was aimed to at the limiting shear strength specified in ACI 318, while the

design joint shear in other four cruciform specimens were designed to exceed the limiting value of $1.25\sqrt{f'_c}$ MPa for interior joints without transverse beams.

Joint transverse hoops and ties are proportioned according to ACI 318 code, which requires special transverse reinforcement to be extended throughout the joint and adjacent column ends, unless a joint is considered to be effectively confined by beams on all four sides, such as Specimens A3 and B3.

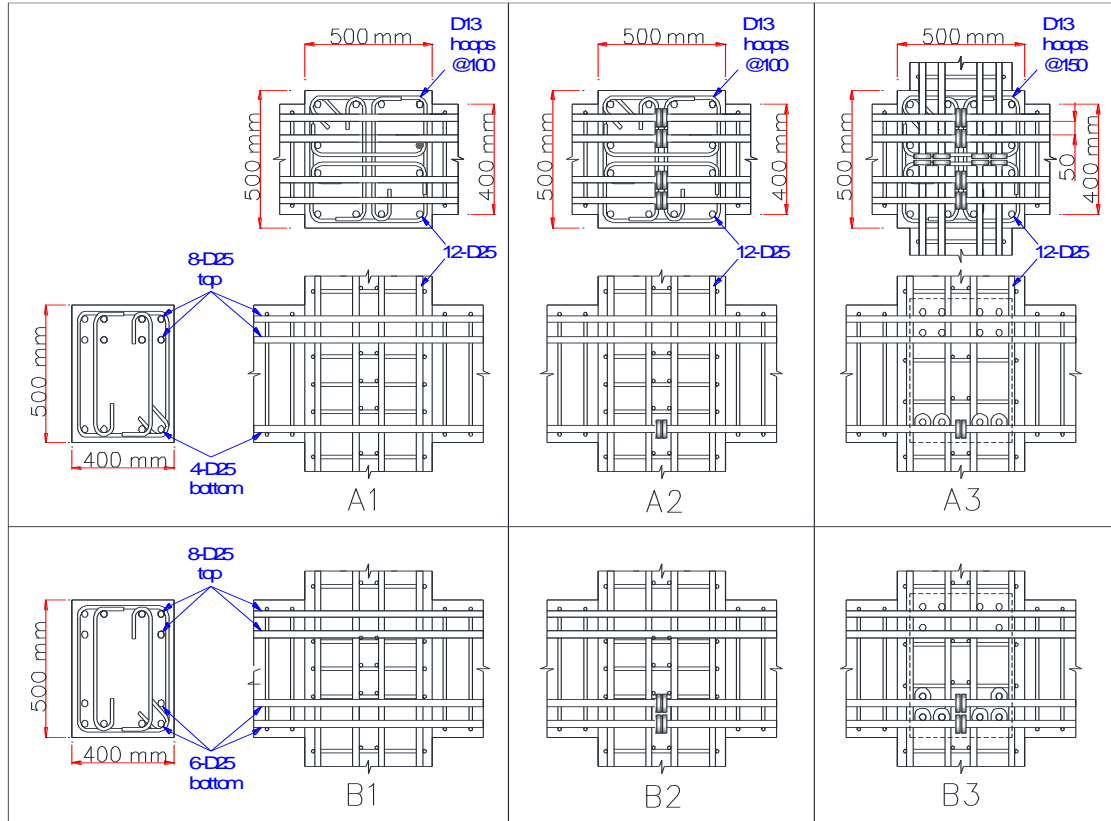


Figure 3. Test matrix of beam-column joint specimens.

Table 1. Material properties and connection design parameters.

Specimen	A1	A2	A3	B1	B2	B3
Concrete strength f'_c (MPa)	56.8	61.9	49.2	55.6	51.2	53.2
Flexural strength ratio M_r^*	1.27	1.28	1.26	1.27	1.27	1.27
Target joint shear V_u (kN)	2717	2717	2717	2721	2721	2721
Confinement ratio $\frac{A_{sh}^{**}}{s b_c}$	0.0112	0.0112	0.0075	0.0112	0.0112	0.0075
Trans. beam confinement	NA	NA	Yes	NA	NA	Yes

*Column-to-beam flexural strength ratio = $\Sigma M_{nc} / \Sigma M_{nb}$, where ΣM_{nc} and ΣM_{nb} are the sum of the nominal moment strengths of the columns and beams, respectively, calculated at the joint faces.

**Where A_{sh} is the total cross-sectional area of the transverse reinforcement, including crossties, within spacing s and perpendicular to dimension b_c , which is the cross-sectional dimension of the column core without concrete cover.

For Grade 420 straight beam bars passing through the joint, ACI 318 and ACI 352R-02 require a minimum column depth of 20 bar diameters ($20d_b$) for joints of special moment frames. All test connections shown in Figure 3 used Grade 420 25-mm-diameter longitudinal reinforcing bars and a

column depth of 500 mm, which is approximate to $20d_b$. For headed deformed bars anchored in the joints of special moment frames, ACI 318 gives a minimum development length, measured from the beam-column interface to the bearing face of the head, as follows.

$$\ell_{dt} = 0.19f_y d_b / \sqrt{f'_c} \quad (3)$$

with limitations of (a) specified f_y not exceeding 420 MPa; (b) bar size not exceeding 36 mm; (c) normal-weight concrete; (d) Each head has a net bearing area exceeding 4 times the nominal cross-sectional area of the bar; (e) minimum clear cover of $2d_b$ for each bar; and (f) minimum clear spacing of $3d_b$ between parallel bars.

Substituting bar f_y of 420 MPa and design concrete strength f'_c of 55 MPa into Eq. (3) resulting in a minimum development length of $10.8d_b$. The provided development length of the headed bars is only $9d_b$, measured from the bearing face of the head to the column face. Furthermore, all test specimens were detailed with longitudinal beam bars at a clear spacing of $2d_b$ between bars. Obviously, the anchorage conditions of the bottom beam bars used in this test program are relatively severe.

Kang et al. (2009) extensively reviewed previous research on the use of headed bars in reinforced concrete beam-column joints and concluded that the minimum clear spacing between headed bars can be reduced to $2d_b$. Also, the ℓ_{dt} of Eq. (3) is relatively much more conservative for headed bars in beam-column joints. Four exterior beam-column joint specimens with staggering headed bars at a clear spacing of $1.2d_b$ tested by Lee and Yu (2007) did demonstrate adequate anchorage capacities. Based on prior experimental evidence, this study used $2d_b$ for headed bar spacing.

2.2 Test setup and procedure

Figure 4 shows the setup for the reversed cyclic loading test of an isolated cruciform beam-column assemblage. The column base was pin-connected on strong floors. At the beginning of test, a column axial load of $0.05A_g f'_c$ was applied via four pretension rods aside the column. During testing, the column axial load was manually held around the target value of $0.05A_g f'_c$. The free ends of the beams were tied down to the strong floor to simulate the inflection points of the beam. The test setup was arranged to eliminate the P-delta effect and to simulate a 3/4-scale beam-column joint specimen with a column height (story height) of 3 m and a beam span of 4.5 m (the distance between the roller-supported inflection points).



Figure 4. Test set-up photo.

A typical displacement-controlled loading protocol consisting of three reversed cycles at gradually increased drift ratios (0.50%, 0.75%, 1.0%, 1.5%, 2%, 3%, 4%, 6%, and 8%) was used in this study. The target displacement at the loading point of the upper column was computed by multiplying the target drift ratio to the simulated story height of 3000 mm. The axial load and lateral force at the upper column were monitored by load cells. Several displacement transducers were attached to the test specimen to measure the global lateral drifts and local deformations. Numerous strain gauges were pre-attached to reinforcements at key locations to record the strain histories. In general, the loading protocol and test

procedure in this experimental program are consistent with respect to ACI 374.1-05(ACI Committee 374, 2005). The presented test results herein continued up to 6% or 8% drift ratio for the observation of failure modes. However, the performance of test specimens should be evaluated prior to the limiting drift ratio of 4%, because the 6% or 8% drift may be too large for a well-designed special moment frame.

3 TEST RESULTS AND DISCUSSION

3.1 Cyclic loading response

Figure 5 shows the hysteretic, skeleton, and backbone curves for all test specimens. Specimens A1 and B1 are benchmark specimens with continuous bottom beam bars. The yielding of beam bars occurred in the cycle of 1.5% drift, followed by the maximum loads measured at the drift ratio of 3% and the significant joint distortion. The applied lateral load (Q) was normalized to the theoretical lateral resistance (Q_n) obtained from measured material properties and a strain compatibility analysis for flexural strengths of the beams at critical section. As shown in Figure 5, the maximum lateral resistances recorded in Specimens A1 and B1 were greater than Q_n , but fall below Q_n at the 6% drift cycles due to the joint shear failure. The failure mode of Specimens A1 and B1 was joint shear failure after beam yielding.

Specimen A2 and B2 exhibited similar behavior and failure modes with respect to Specimen A1 and B1. As compared in Figures 6 and 7, the cyclic response of Specimen A2 was almost identical to that of Specimen A1. On the other hand, the performance of Specimen B2 was somewhat inferior to that of Specimen B1. Based on testing observation and comparison, it is concluded that the proposed alternative details for bottom beam bars can be used if following conditions were satisfied. Firstly, the ratio of bottom-to-top flexural reinforcement is about 0.5. Secondly, the joint is well confined with joint transverse reinforcement. Finally, the anchorage length of the headed bars should be sufficient to preclude the breakout failure.

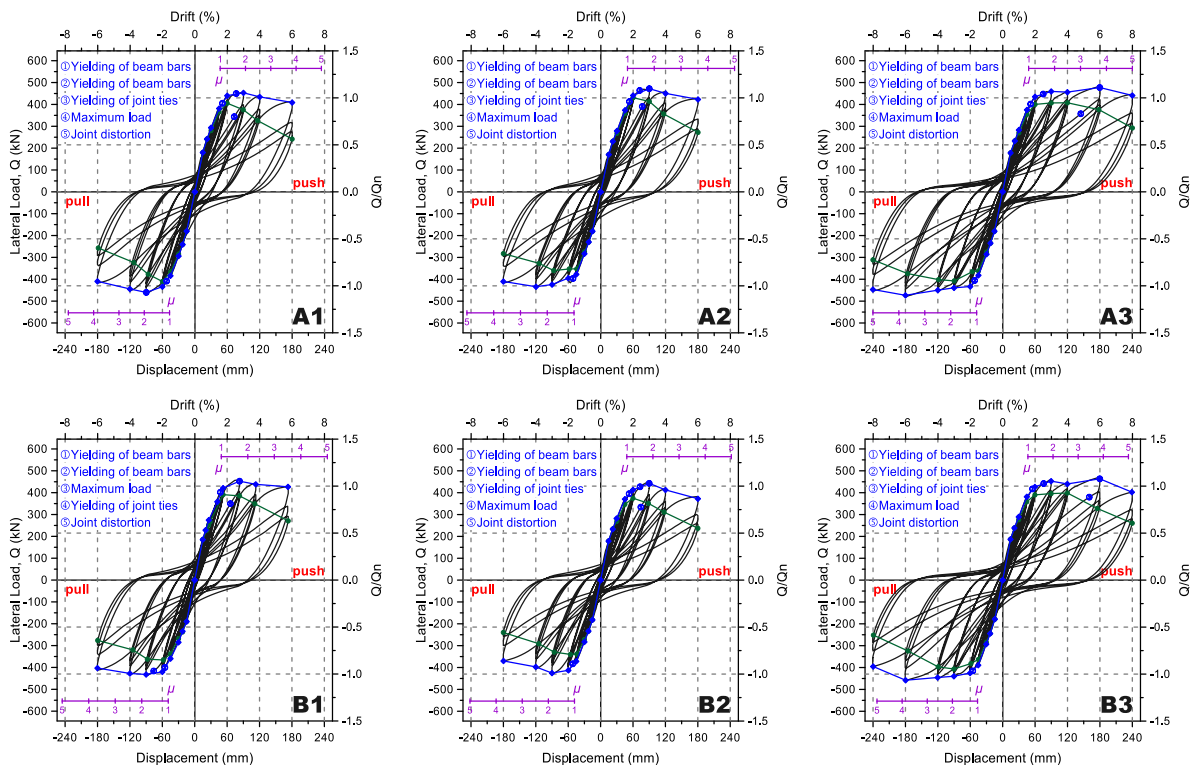


Figure 5. Hysteretic, skeleton, and backbone curves of tested units.

As shown in Figures 5, the performance of Specimens A3 and B3, which were confined on all four faces, were obviously better than those of other four cruciform specimens. Due to the enhancement of transverse beams to the joint, Specimens A3 and B3 attained the maximum lateral resistances at the drift ratio of 6%, which is more than enough for a well-designed moment resisting frame. The cyclic loading

tests of Specimens A3 and B3 were therefore continued to finish the 8% drift ratio to observe failure modes. Figure 6 shows the final damage stage of Specimen B2 at the end of 6% drift cycles and that of Specimen B3 at the end of 8% drift cycles. Due to the confinement of the transverse beams, the joint damage in Specimen B3 is less than that in Specimen B2. On the other hand, Specimen B3 had well-developed beam plastic hinges adjacent to the joint.



Figure 6. Final damage patterns of Specimen B2 and B3.

3.2 Anchorage performance of bottom beam bars

Figure 7 shows the strain profiles along the bottom beam bars at peak drift ratios for the four cruciform specimens. All beam bar strains measured at the beam-column faces (location at ± 250 mm) went above the ideal yield strain of $2155 \mu\epsilon$ (measured from bar tensile test) at the 2% drift ratio indicating the development of beam yielding. For Specimen A1 and B1, a clear strain gradient per distance along the straight beam bar passing through the joint can be observed in Figure 7. This indicated that the bond resistance in the joint had not been completely destroyed till the 3% drift ratio. It is concluded that the development length of $20d_b$ is adequate for the straight beam bars used in the test specimens.

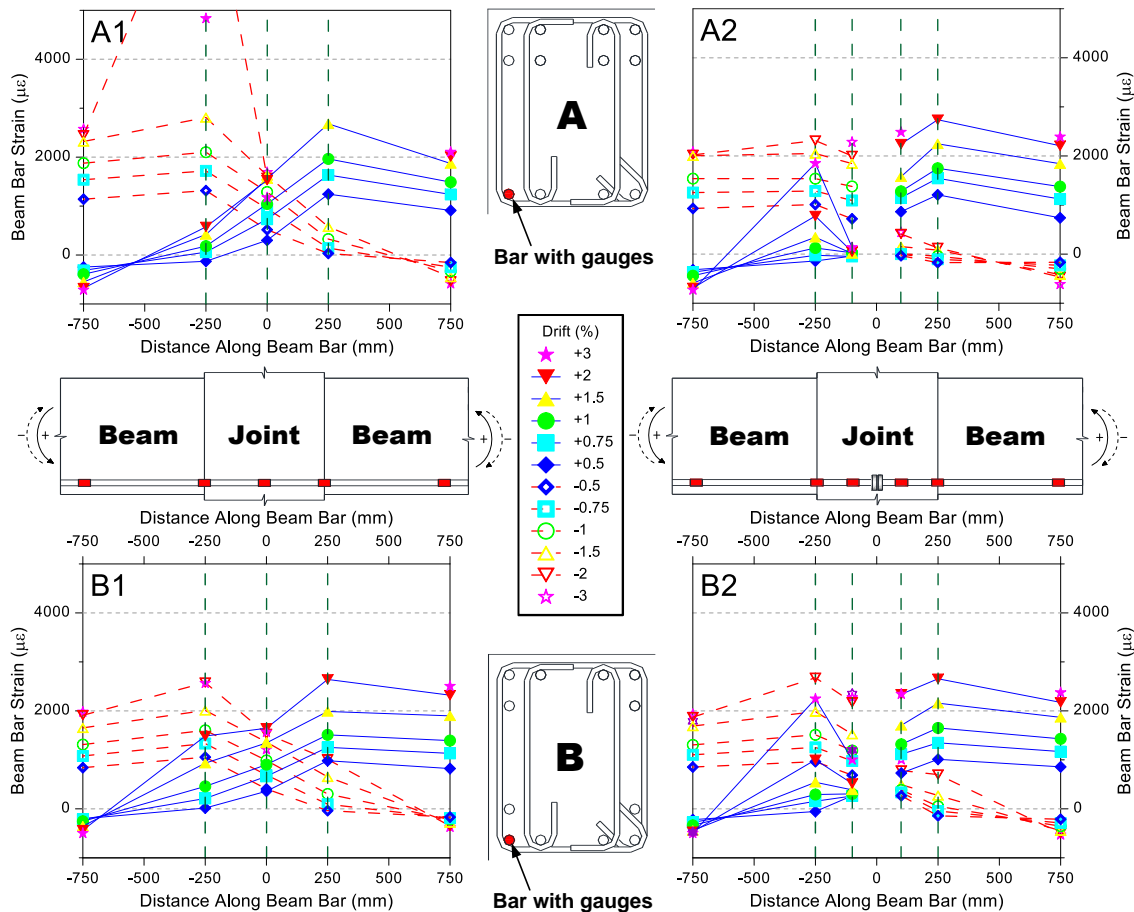


Figure 7. Profiles of strain developed along bottom beam bars for test specimens.

For Specimens A2 and B2 with alternative reinforcing details, the beam bar strains measured at the beam-column faces (location at ± 250 mm) and in the joint core (location at ± 100 mm) exceeded the bar yield strain at the 2% drift ratios indicating almost the entire bar tensile force was transferred to the end anchorage. It is evident that the bottom beam bars in Specimen A2 and B2 were effectively anchored by heads with a short anchorage length and a clear spacing of $2d_b$ in the beam-column joints. Notably, the joints were well detailed with transverse reinforcement.

3.3 Profiles of tie bar stress

Figure 8 compares the profiles of tie bar strains measured at one top column crosstie (Gauge 11) above the top beam bars, three inner joint crossties (Gauges 12-14) between the top and bottom beam bars, and another bottom column crosstie (Gauge 15) below the bottom beam bars for the cruciform test specimens. Each gauge was attached to the centre of the crosstie parallel to the beam bars. Figure 8 shows that the tie bar strains measured in the joint (Gauges 12-14) remained elastic in the 1.5% drift cycles but went beyond the yield strain of $2500 \mu\epsilon$ at the 2% drift ratios for all test specimens. Notably, the tie bar strains measured in the top and bottom column (Gauges 11 and 15) remained elastic over the entire loading history in Specimens A1 and B1 with continuous bottom beam bars.

In contrast, the tie bar strains measured below the discontinuous bottom beam bars in Specimens A2 and B2 (Gauge 15) went beyond the yield strain of $2500 \mu\epsilon$ after the 2% drift cycles. Besides, the tie bar strain of Gauge 14 in Specimen B2 was relatively larger than that of Gauge 14 in Specimen B1 for each drift level. These phenomena can be explained using Figure 9, where the tensile force of the bottom beam bars was transferred to the transverse reinforcement in the joint and the bottom column.

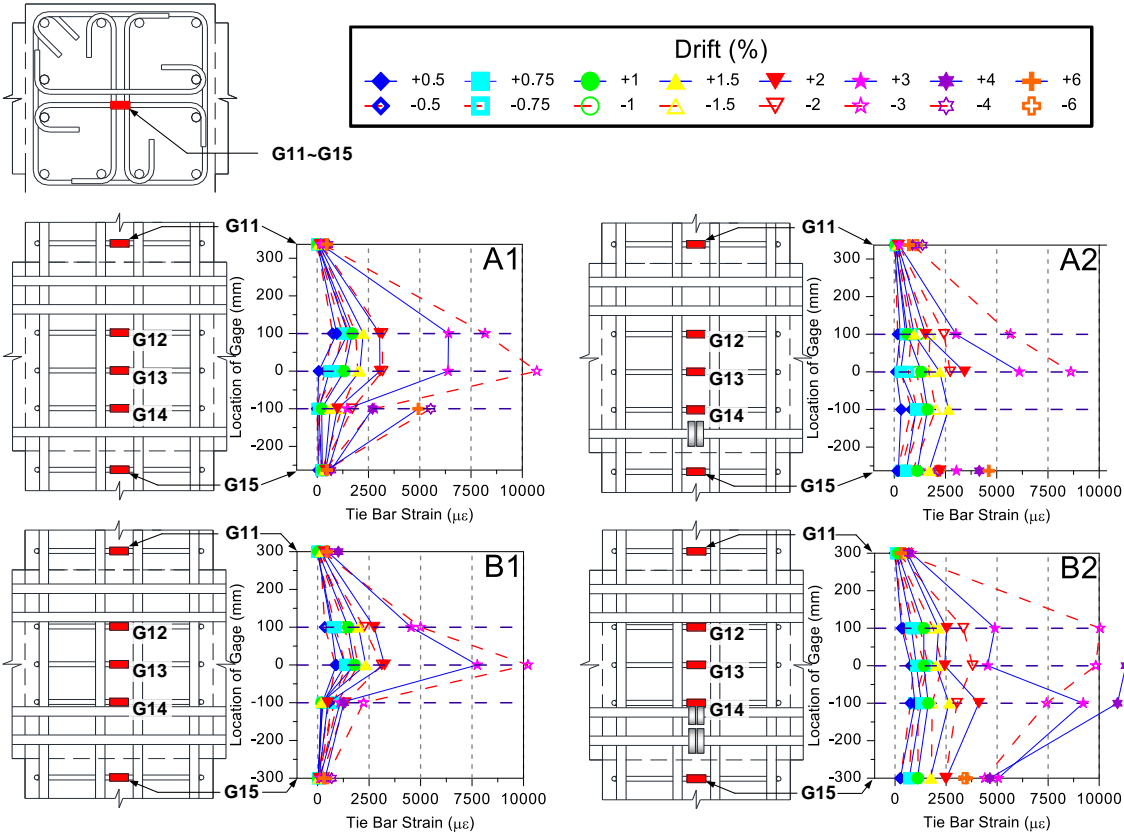


Figure 8. Profiles of tie bar strain along column height.

4 DESIGN RECOMMENDATIONS

For the anchorage of the bottom beam bars by heads in the middle of the joint, yielding of the column transverse reinforcement is not preferred because it may affect the column confinement. Therefore, it is recommended to provide one more set of joint transverse reinforcements below the bottom beam bars anchored in the joint, as shown in Figure 9. To preclude breakout failure, this paper recommends that

the total amount of joint and column transverse reinforcement covered by the fan-shaped struts should be capable of resisting the total tensile force to be developed in the bottom beam bars.

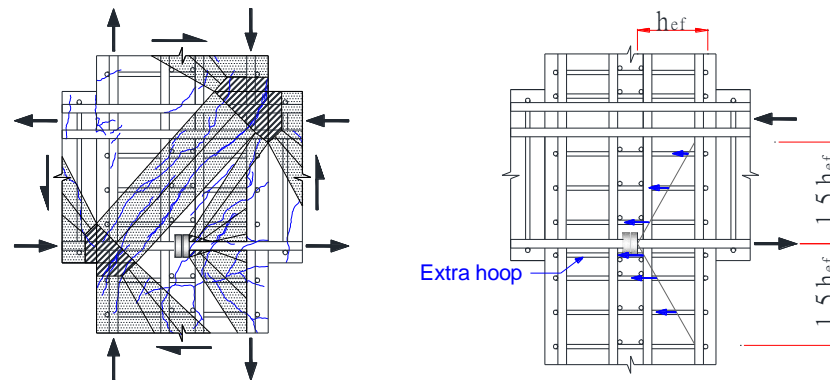


Figure 9. Strut-and-tie modelling for precluding the concrete breakout failure.

5 CONCLUSIONS

The experimental results presented in this work demonstrated that emulative precast beam-column connections with bottom beam bars anchored in the joint middle can perform as well as monolithic beam-column connections with straight beam bars passing through the joint. Based on standard testing protocol and performance evaluation, it is concluded that it is a viable option to terminate bottom beam bars at the middle of a well-confined joint with adequate heads, practical clear spacing of $2d_b$, and sufficient anchorage length. From the experimental observations, the potential for concrete breakout failure increased for the closely spaced headed bars that were used in the test specimens. To preclude breakout failure, adequate transverse reinforcement should be provided and distributed uniformly within the critical edge distance of 1.5 times the effective embedded depth of the headed bars in the confined core. The amount of transverse reinforcement could be proportioned by establishing load paths in accordance with strut-and-tie modelling principles.

6 REFERENCES

- ACI-ASCE Committee 352. 2002. *Recommendations for Design of Beam-Column Connections in Monolithic Reinforced Concrete Structures (ACI 352R-02)*. Retrieved from Farmington Hills, MI:
- ACI Committee 318. 2014. *Building Code Requirements for Structural Concrete (ACI 318-14) and Commentary*. Farmington Hills, MI: American Concrete Institute.
- ACI Committee 374. 2005. *Acceptance Criteria for Moment Frames Based on Structural Testing and Commentary (ACI 374.1-05)*. Retrieved from Farmington Hills, MI:
- Kang, T.H.K., Shin, M., Mitra, N., & Bonacci, J.F. 2009. Seismic Design of Reinforced Concrete Beam-Column Joints with Headed Bars. *ACI Structural Journal*, 106(6), 868-877.
- Lee, H.J., & Yu, S.Y. 2009. Cyclic Response of Exterior Beam-Column Joints with Different Anchorage Methods. *ACI Structural Journal*, 106(3), 329-339.
- Pampanin, S. 2005. Emerging solutions for high seismic performance of precast/prestressed concrete buildings. *Journal of Advanced Concrete Technology*, 3(2), 207-223.
- Park, R. 2002. Seismic Design and Construction of Precast Concrete Buildings in New Zealand. *PCI Journal*, 47(5), 60-75.
- Wallace, J.W., McConnell, S.W., Gupta, P., & Cote, P.A. 1998. Use of headed reinforcement in beam-column joints subjected to earthquake loads. *ACI Structural Journal*, 95(5), 590-606.
- Watanabe, F. 2007. Design of Precast Concrete Buildings Emulating Monolithic Construction. *Proceeding of The Ninth Japan-Korea-Taiwan Joint Seminar on Earthquake Engineering for Building Structures (SEEBUS 2007)*, Hsinchu, Taiwan.

Database investigation on bond performance of interior beam-column joints with high-strength reinforcement

H.C. Chen

Graduate School of Engineering Science and Technology, National Yunlin University of Science and Technology, Yunlin, Taiwan.

H.J. Lee & T.C. Tsai

National Yunlin University of Science and Technology, Yunlin, Taiwan.



2017 NZSEE
Conference

ABSTRACT: The use of high-strength reinforcement in concrete structures has many advantages such as labor and cost savings. Whenever higher strength reinforcement is used, the bond and development length becomes critical problems for design of concrete structures, especially for joints of moment-resisting frames. This paper reviewed existing design criteria of development length for the straight beam bars within beam-column joints and recommended to extend the bond requirements of NZS 3101 for the use of Grade 690 reinforcing bars. According to an extensive database investigation, the validity of the design equations of NZS 3101 is assessed by hysteresis performance of beam-column joint tests collected from laboratories in Unites States, Japan, New Zealand, and Taiwan. Practical design recommendations are drawn for Grade 690 reinforcing bars being use as longitudinal reinforcement passing through joints of moment-resisting frame.

1 INTRODUCTION

Special moment-resisting frames are widely used for the design of reinforced concrete building structures in moderate to high seismic zones. If properly detailed, the plastic hinge can be arranged to develop at the beam regions adjacent to the joint when the frame subjected to large lateral loads, as shown in Figure 1(a). During the formation of these beam plastic hinges, extremely high bond stresses can be developed along the straight beam bars passing through the joint, because these bars may be forced to yield in tension at one column face and be close to yield in compression at the opposite column face. Once certain degree of bond deterioration occurred within the joint, these beam bars may slip within the joint under large load reversals.

Significant bond slip is not desirable because it reduces the stiffness and energy dissipation capacity of beam-column connections. Some bond deterioration is inevitable and should be accepted. However, if the bond deterioration is severe, the bar tension will penetrate through the joint and develop in the beam compression zone on the opposite side. This means that both top and bottom beam bars are in tension at the column face and then large compression forces will transfer to the concrete of the beam compression zone. As shown in Figure 1(b), concrete crushing at beam ends may occur consequently and followed by significant reduction on beam flexural strength and ductility. Hakuto et al. (1999) ever demonstrated the detrimental effect of bond deterioration by analytical studies and concluded that bond deterioration should be considered in the design of beam-column joints.

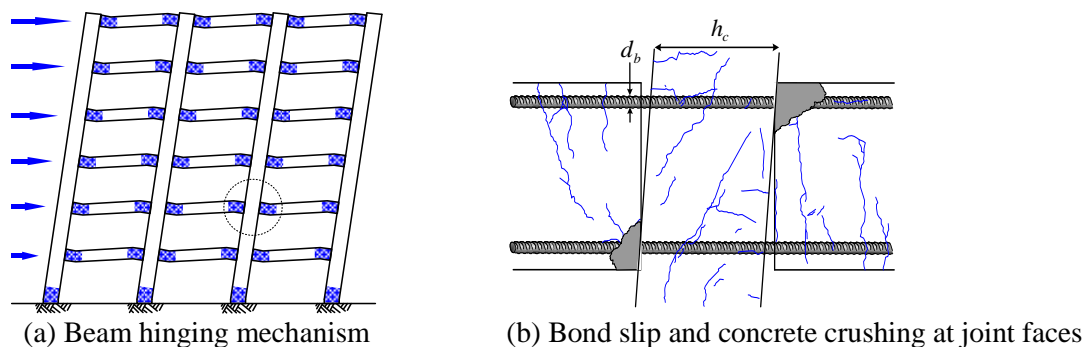


Figure 1. Bond failure at interior beam-column joints for earthquake resistance.

Although bond performance of beam bars passing through interior joints have been extensively studied since 1980s, the development length requirements for beam-column joints still differ remarkably among the current ACI 318 Code (ACI 318 2014) in United States, the AIJ Guideline (AIJ 1999) in Japan, and the NZS 3101 Standard (NZS 3101 2006) in New Zealand. For seismic design of interior beam-column joints in special moment-resisting frames with normal weight concrete, the ACI 318 Code requires a minimum column dimension of 20 times the largest diameter of beam bars parallel to that column dimension. This criterion was based on an evaluation of available tests in 1980s. Zhu and Jirsa (1983) reviewed cyclic loading response of 18 interior beam-column joints with normal strength concrete and reinforcement. While ACI 318 Code set a simple criterion of 20-bar diameters, both the AIJ Guideline and the NZS 3101 Standard establish the minimum ratios of column dimension to beam bar diameter as a function of material strengths and the column axial stress. The philosophy behinds these requirements are based on elaborate studies on the energy dissipation capacities of beam-column joints in Japan and New Zealand.

High-strength concrete has been used in many building structures in Japan (Aoyama 2001), particularly, for columns with limited architectural dimensions and high axial load at the lower levels. Whenever high-strength reinforcement is used for beam longitudinal reinforcement passing through a beam-column joint, either a large column depth or a small permissible diameter of beam bars would make design and proportion difficult. To provide a promising solution, this paper compares existing bond requirements in international concrete design codes and then validates proper design equations using a large database of beam-column joint tests. Laboratory testing performances such as strength, stiffness, and energy dissipation capacity of each beam-column joint specimen are evaluated according to ACI standards (ACI 374 2005) for special moment frames. Finally, a viable set of design equations for the development length in beam-column joints is recommended to achieve acceptable bond performance for special moment frames.

2 EXISTING DESIGN CRITERIA

2.1 Genetic formula

For the use of Grade 500E reinforcement in New Zealand, Brooke and Ingham (2013) reviewed existing design criteria for the reinforcement anchorage length at interior beam-column joints. During the formation of the adjacent beam hinging, the stresses on the beam bar may achieve $\alpha_o f_y$ in tension at one face of the joint and $\kappa \alpha_o f_y$ in compression at the opposite face of the joint, as shown in Figure 2.

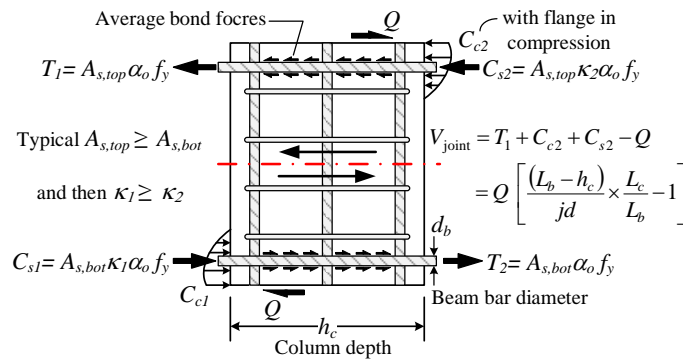


Figure 2. Horizontal shear and bond forces acting on the joint concrete.

By assuming an average bond stress on the beam bar along the column depth, the bond requirements for preventing excessive bond slip of beam bars in joints are given as follows.

$$\pi d_b h_c \alpha_p u_b \geq \frac{\pi d_b^2}{4} \alpha_o f_y (1 + \kappa) \quad (1a)$$

$$\frac{h_c}{d_b} \geq \frac{(1 + \kappa) \alpha_o f_y}{4 \alpha_p u_b} \quad (1b)$$

where h_c = column depth; d_b = maximum bar diameter of the beam bars passing through the joint; f_y = is

specified yield strength of the reinforcement; u_b = average bond stress on the beam bar in the joint; α_p = factor accounting for the benefit effect of column axial compression on bond strength; α_o = overstrength factor of the beam bars; and κ = ratio of bar compressive stress to the bar tensile stress.

2.2 Existing design equations

Bond requirements on the basis of Eq. (1) can be found in AIJ Guideline (AIJ 1999) and NZS 3101 (NZS 2006). Table 1 compares above design criteria with the design recommendations proposed by Brooke and Ingham (2013) and this paper. Among the existing design criteria, differences can be found for the $(1 + \kappa)$ term of bar stress being developed in the joint, average bond strength u_b along the bar, and the factor α_p of the column axial stress on bond strength. Originally, NZS 3101 uses an average bond strength of $1.5\sqrt{f'_c}$ MPa, which is 60% of the peak local bond strength of $2.5\sqrt{f'_c}$ MPa observed by Eligehausen et al. (1983), and two additional modification factors, α_f and α_t , to consider the bidirectional loading and the top bar effects, respectively. Paulay and Priestley (1992) described detail development of above α factors.

Recently, Brooke and Ingham (2013) assembled a database of 93 interior beam-column joint tests to assess the suitability of existing design criteria for the bond development length in joints and concluded that the existing criteria cannot reflect the bond failure observed in experiments. They proposed to modify the basic bond strength from $1.5\sqrt{f'_c}$ to $1.25\sqrt{f'_c}$ MPa and the corresponding equations of κ and α_p for updating NZS 3101, as shown in Table 1. The α_p factor proposed by Brooke and Ingham (2013) is relatively conservative with a upper limitation of 1.20 for high axial load conditions. Following prior investigation, this paper recommends to omit the α_f and α_t terms and set the bond strength $u_b = 1.5\sqrt{f'_c}$, which are demonstrated with satisfactory bond performance in laboratory testing.

Table 1. Comparison of existing design equations for the development length in interior joints.

Design criteria	Bar stress factor $1 + \kappa$	Bond strength u_b (MPa)	Axial stress factor $\alpha_p \geq 1.0$
AIJ 1999	$1 + \frac{A_{s,bot}}{A_s}$	$0.7(f'_c)^{2/3}$	$1 + \frac{P}{A_g f'_c}$
NZS 3101	$1 + 1.55 \frac{A_s}{A_{s,top}} \leq 1.8$	$\alpha_f \alpha_t 1.5\sqrt{f'_c}$	$0.95 + 0.5 \frac{P}{A_g f'_c} \leq 1.25$
Brooke & Ingham 2014	$1 + \frac{0.7 A_{s,top}}{\alpha_o A_s} \leq 1 + \frac{1}{\alpha_o}$	$\alpha_f \alpha_t 1.25\sqrt{f'_c}$	$0.9 + 2.0 \frac{P}{A_g f'_c} \leq 1.20$
Recommended	$1 + \frac{0.7 A_{s,top}}{\alpha_o A_s} \leq 1 + \frac{1}{\alpha_o}$	$1.5\sqrt{f'_c}$	$0.9 + 2.0 \frac{P}{A_g f'_c} \leq 1.20$

Note: With limitation of $A_{s,top} \geq A_{s,bot}$, where $A_{s,bot}$ = area of bottom beam bars; $A_{s,top}$ = area of top beam bars; A_s = area of the bar group, $A_{s,top}$ or $A_{s,bot}$, containing the bar for which development length is being calculated; α_o = overstrength factor for beam bars; $\alpha_f = 1.0$ for a beam bar passing through a joint subjected to unidirectional loading, and $\alpha_f = 0.85$ for bi-directional loading; Bar location factor $\alpha_t = 0.85$ for a top beam bar where more than 300 mm of fresh concrete is cast below the bar, $\alpha_t = 1.0$ for all other cases. P = axial compression force on column; A_g = gross area of column; f'_c = concrete compressive strength.

For many years, Grade 420 ($f_y = 420$ MPa) steel reinforcement has been the standard for reinforced concrete construction in Taiwan as well as in the United States. Whenever high-strength steel reinforcing bars are used in the concrete structures, bond requirements become critical issues for design and proportion. ACI-ASCE Committee 352 (2002) recommends a reasonable multiplier of $f_y/420$ MPa for the minimum column depth of $20d_b$ for higher grade reinforcement.

$$\frac{h_c}{d_b} \geq 20 \frac{f_y}{420} \quad (2)$$

For comparison of the existing design equations, a reference cruciform beam-column joint is assumed to have beam hinging adjacent to the joint faces, a least axial compression of $0.2A_g f'_c$, a practical beam reinforcement ratio $A_{s,bot}/A_{s,top}$ of 0.75, equal bar diameter for top and bottom reinforcement, and bar f_y of 420 or 690 MPa. Under such conditions, the minimum column depths with respect to the bottom bar diameter are compared in Figure 3. Clearly, the bond requirements of AIJ Guideline (1999) are very conservative, and those of NZS 3101 are relatively less conservative. The recommendations of Brooke and Ingham (2013) still results in a column depth similar to those of NZS 3101 (2006). The minimum column depth recommended by ACI 352R (2002) is also displayed in Figure 3, which may be conservative for normal strength concrete but be too conservative for high strength concrete.

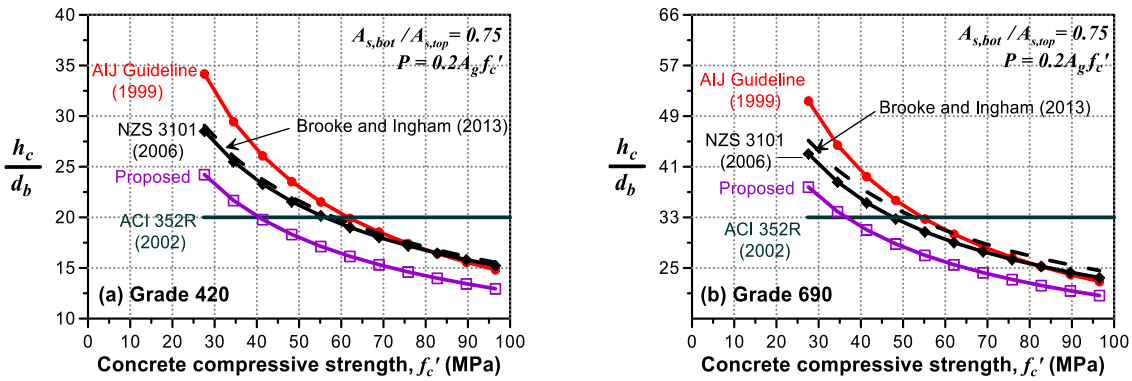


Figure 3. Comparison of minimum column depth for (a) Grade 420 bars with $\alpha_o = 1.25$; (b) Grade 690 bars with $\alpha_o = 1.15$.

3 DATABASE INVESTIGATION AND PERFORMANCE EVALUATION

3.1 Database of beam-column joint tests

Lee and Hwang (2013) presented a database for reverse cyclic tests of reinforced concrete beam-column joints in special moment frames by extensively reviewing the related papers published in Japan, United States, New Zealand, and Taiwan. About 200 interior joints were assembled in this database. All specimens were reinforced concrete concentric beam-column subassemblages isolated from inflection points of beams and columns, and tested under quasi-static cyclic lateral loading (typical repeated cycles for each drift ratio ranged from one to three) to simulate the earthquake-introduced forces acting on the joints.

Test results of beam-column joints were classified in three basic failure modes including: Beam flexure failure (“B” failure), Joint shear failure without yielding of beam bars (“J” failure), Joint shear failure with yielding of beam bars (“BJ” failure). The modes of B-, BJ-, and J-failures are well-accepted in Japan for the development of design guidelines for beam-column joints (Kitayama et al. 1991). Besides above three basic failure modes, some joint specimens were reported as BJa failure, which is refer to bond or anchorage failure along the beam bars in the joint.

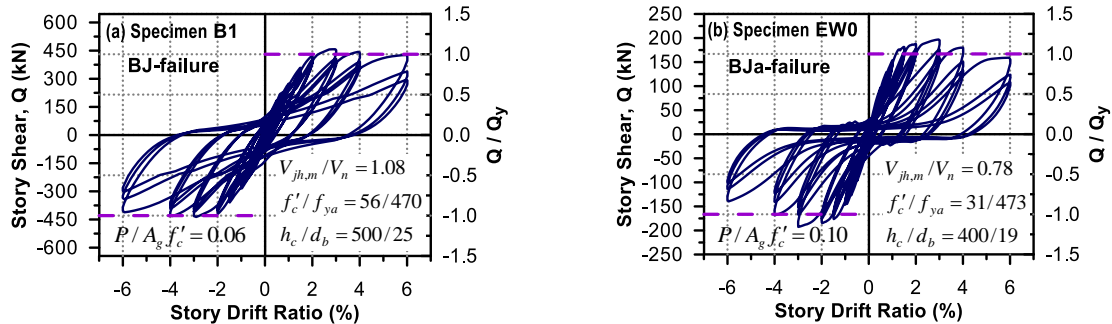


Figure 4. Cyclic loading response of (a) BJ-failure and (b) BJa-failure joint specimens tested in YunTech.

Figure 4 shows two interior beam-column joints tested by first authors and his colleagues at YunTech in Tawian. Both specimens reached beam yielding at about 1.5% to 2% drift ratio, but Specimen B1 eventually failed in joint shear at 6% drift ratio while Specimen EW0 exhibited a very pinched hysteretic curve since the bond failure occurred in the 3% drift cycles. Notably, both specimens had a column depth of 20 bar diameters and similar bar yield strength, but hysteresis performance of the Specimen B1 is better than that of Specimen EW0, although the later had a lower target shear stress in the joint. Obviously, the key parameter make Specimen B1 perform better is attributed to its higher concrete strength (greater bond resistance in the joint).

It seems the hysteresis performance of beam-column joints is also related to the bond stress of the beam bar in the joint. Although the consequence of bond failure is not as severe as that of shear failure in joints, it is still preferred to prevent the bond failure within the design earthquake level, which is about 3.5% drift capacity for the structural testing. This paper intends to determine a viable set of design equations to cover the use of Grade 690 reinforcement in joints of special moment frames. Therefore, a subset of available test data from the database of Lee and Hwang (2013) was investigated in this paper according to ACI 374.1-05, the acceptance criteria for moment frames (ACI Committee 374, 2005). Hysteretic performances including strength, stiffness, and energy dissipation capacity for each test specimen were evaluated for assessing existing design codes and recommendations for the development length in beam-column joints.

3.2 Acceptance criteria for testing performance of beam-column joints

ACI Committee 374 (2005) reported a testing protocol and acceptance criteria for structural components of special moment frames. For acceptance, test results of the third complete cycle to a limiting drift ratio not less than 3.5% should satisfy:

1. Strength at peak displacement shall not be less than 75% of the maximum peak strength in the same loading direction;
2. Secant stiffness between drift ratios of $-1/10$ and $+1/10$ of the limiting drift ratio shall not be less than 5% of the initial stiffness obtained from the first cycle; and
3. Energy dissipation in the third cycle of limiting drift ratio shall not be less than 12.5% of the idealized elastoplastic energy of that drift ratio.

For Specimen EW0 shown in Figure 4(b), the third 4% drift cycle had a peak strength equal to 64% of the maximum peak strength, a secant stiffness between $\pm 0.4\%$ drift ratios equal to 1% of the initial stiffness, and an relative energy dissipation ratio of 19%. Obviously, hysteresis performance of Specimen EW0 is not acceptable because it does not satisfy the three acceptance criteria given by ACI 374.1-05. The poor hysteresis performance of Specimen EW0 can be attributed to the bond failure along beam bars in the joint occurred in 3% drift cycles.

The selection of number of cycles at each drift ratio depends on the judgment of the researchers and the particular degradation characteristics of the system being tested. More recently, ACI 374.2R-13 (ACI Committee 374 2013) reported that a minimum of two cycles at each deformation level is sufficient to consider the damage associated with the number of cycles at a given drift level. For the assessment of the bond performance for each test specimen, therefore, the second (or third, if available) cycle at a drift ratio between 3.5% and 4% were reproduced. Therefore, this paper selected 59 interior joints from the database of Lee and Hwang (2013) according to following conditions:

- BJ or BJa failure specimens;
- straight beam bars passing through the joint with bar f_y exceeding 400 MPa;
- cyclic loading response have a minimum of two cycles at a drift ratio exceeding 3.5%.

After screening, a total amount of 65 interior joint specimens (46 BJ and 19 BJa data) are evaluated in this paper. Figure 5 displays the range of measured concrete strength and bar yield strength for the selected BJ and BJa failure specimens. Obviously, bond failure is likely to occur for the combination of higher strength reinforcement and normal-strength concrete. Within the test database, there is no BJa-failure specimens available for concrete strength exceeding 100 MPa.

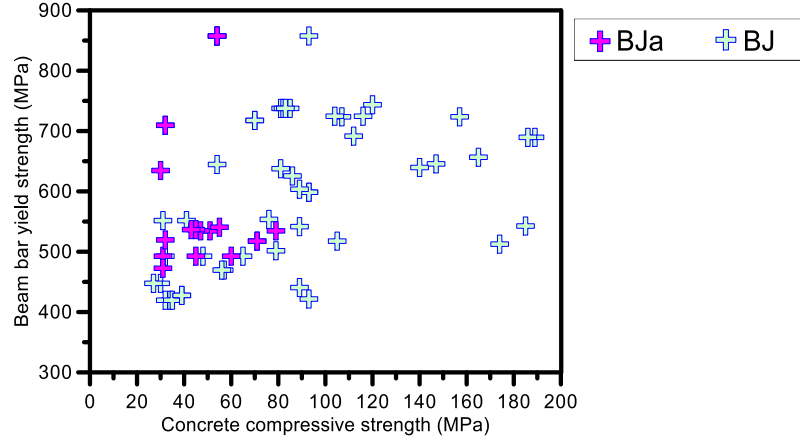


Figure 5. Range of joint concrete strength and bar yield strength in the selected subset of test data.

3.3 Assessment of bond requirements

According to the three acceptance criteria given by ACI 374.1-05, the second (or third, if available) cycle at a drift ratio about 4% for each test specimen is evaluated and classified as “acceptable” or “unacceptable” performance. The acceptable test data satisfy the aforementioned three acceptance criteria while the unacceptable may only meet one or two of the three acceptance criteria.

Figure 6(a) shows the relations of hysteresis performance to the ratio of experimental-to-nominal joint shear strength and the ratio of provided-to-required column depth. The vertical axis of Figure 6 is the maximum experimental joint shear force ($V_{jh,m}$), which can be back-calculated from the beam moments in equilibrium with the peak maximum lateral loads, divided by the nominal joint shear strength ($V_n = 1.25\sqrt{f'_c}A_j$) specified in ACI 318 (2014) for interior joints without transverse beams. Therefore, test data fall in Quadrant 3 and 4 had experimental joint shear stresses below the permissible value of $1.25\sqrt{f'_c}$ MPa and expected to be capable of precluding the premature shear failure.

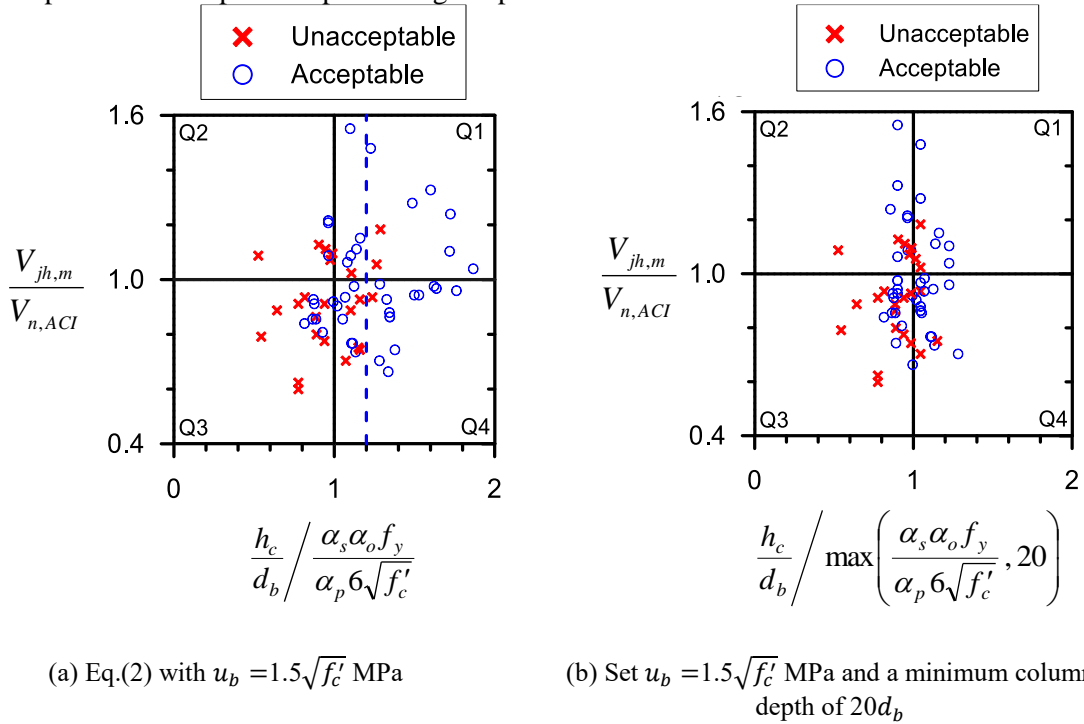


Figure 6. Relations of hysteresis performance to the ratio of experimental-to-nominal joint shear strength and the ratio of provided-to-required column depth.

The horizontal axis of Figure 6(a) is provided column depth in experiments divided by the required

column depth recommended in this paper. In other words, test data fall in Quadrant 1 and 4 had column depth exceeding the minimum column depth, calculated using a basic bond strength of $1.5\sqrt{f'_c}$ MPa combined with the factors $(1 + \kappa)$ and α_p proposed by Brooke and Ingham (2013), and expected to be capable of precluding premature bond failure. Ideally, test data with unacceptable performance shall not appear in Quadrant 4 because both the joint shear and bond stress are kept within permissible limits. However, as shown in Figure 6(a), there are six unacceptable data in Quadrant 4, indicating that the use of basic bond strength of $1.5\sqrt{f'_c}$ MPa may be unconservative for certain conditions.

One of the solutions to improve conservation is to reduce the basic bond strength from $1.5\sqrt{f'_c}$ to $1.25\sqrt{f'_c}$ MPa, as proposed by Brooke and Ingham (2013), and then increase 20% of the required column depth, as shown by the vertical dash line in Figure 6(a). Clearly, only one unacceptable test data exceeds 1.20 times the proposed bond development length (vertical dash line). However, many acceptable test data also fall between 1.0 and 1.20 times the proposed bond development length, indicating the reduction of basic bond strength from $1.5\sqrt{f'_c}$ to $1.25\sqrt{f'_c}$ MPa may also be too conservative for some conditions.

Another simple promising way is to improve the safety by setting a minimum column depth of 20 bar diameters instead of reducing the basic bond strength. As shown in Figure 6(b), the limitation of minimum $20d_b$ criterion moves those test data with low $f_y/\sqrt{f'_c}$ ratios toward the left quadrants and substantially improves the distribution of the unacceptable data. According to data observation in Figure 5, it is concluded that either the minimum column depth of $20d_b$ or the reduction of basic bond strength from $1.5\sqrt{f'_c}$ to $1.25\sqrt{f'_c}$ MPa would give similar safety to preclude unacceptable hysteresis performance.

Finally, the minimum column depth proposed herein are based on test data obtained from relatively conservative bond conditions of the beam bars, which extend through an isolated cruciform beam-column joints without transverse beams and slabs. There is lack of experimental evidence of bond failure observed from indeterminate frame with floor slabs, which may counter the slip of beam bars passing through the frame joints. Definitely, a larger h_c/d_b ratio could reduce the potential beam bar slip within the interior joints during a major earthquake, but it would also lead to larger columns and/or smaller diameter bars in groups, which makes design and construction difficult. Therefore, the minimum h_c/d_b ratios specified for special moment frames by codes and standards are based on the judgment of how well the hysteresis behaviour expected at a design interstorey drift is.

After a design earthquake attack, a moment frame with bond failure in joints may be too flexible under a moderate earthquake. Because it is unlikely to be repair bond failure, a beam-column joint has better be well-proportioned to avoid bond failure occurred during a design-based earthquake. Although bond performance of beam bars passing through interior joints have been extensively studied since 1980s, the development length requirements for beam-column joints still differ remarkably among the international design codes and standards. This paper only provides recommendations for joints of special moment frame designed and detailed according to ACI 318 code.

4 DESIGN RECOMMENDATIONS AND CONCLUSIONS

Based on database investigation, this paper recommends a viable set of design equations for the development length of straight beam bars passing through the joints of special moment frame. The proposed design equations are validated by the testing performance of beam-column joints at a drift ratio about 4%, where the hysteresis behaviour is evaluated by the acceptance criteria specified in ACI Code and standards. For achieving an acceptable bond performance, a minimum column depth-to-beam bar diameter ratio can be related to available bond strength in the joint, reinforcement ratio in beams, and column axial loads. Using common bond design equations, it is recommended to use a basic bond strength of $1.5\sqrt{f'_c}$ MPa with two modification factors proposed by Brooke and Ingham (2013), accounting for effects of reinforcement ratio and column axial loads. Besides, the minimum column depth-to-beam bar diameter ratio should not be taken less than 20.

5 REFERENCES

- ACI (American Concrete Institute). 2014. *Building code requirements for structural concrete and commentary*. ACI 318-14, Farmington Hills, MI.
- ACI-ASCE Committee 352. 2002. *Recommendations for design of beam-column connections in monolithic reinforced concrete structures*. ACI 352R-02, American Concrete Institute, Farmington Hills, MI.
- ACI Committee 374. 2005. *Acceptance criteria for moment frames based on structural testing and commentary*. ACI 374.1-05, American Concrete Institute, Farmington Hills, MI.
- ACI Committee 374. 2013. *Guide for testing reinforced concrete structural elements under slowly applied simulated seismic loads*. ACI 374.2R-13, American Concrete Institute, Farmington Hills, MI.
- AIJ (Architectural Institute of Japan). 1999. *Design guidelines for earthquake resistant reinforced concrete buildings based on inelastic displacement concept*, Tokyo (in Japanese).
- Aoyama, H. 2001. *Design of modern highrise reinforced concrete structures*, World Scientific, Singapore.
- Brooke, N. & Ingham, J. 2013. Seismic design criteria for reinforcement anchorages at interior RC beam-column joints. *J. Struct. Eng.*, 10.1061/(ASCE)ST.1943-541X.0000762, 1895-1905.
- Eligehausen, R., Popov, E.P., & Bertero, V.V. 1983. *Local bond stress-slip relationships of deformed bars under generalized excitations*. UCB/EERC-83/23, University of California, Berkeley CA.
- Hakuto, S., Park, R., & Tanaka, H. 1999. Effect of deterioration of bond of beam bars passing through interior beam-column joints on flexural strength and ductility. *ACI Struct. J.*, 96(5), 858-864.
- Kitayama, K., Otani, S., & Aoyama, H. 1991. Development of design criteria for rc interior beam-column joints. *SP-123: Design of beam-column joints for seismic resistance*, American Concrete Institute, Farmington Hills, MI, 97-123.
- Lee, H.J., & Hwang, S.J. 2013. High-strength concrete and reinforcing steel in beam-column connections. *Proc., Structures Congress 2013*, ASCE, Pittsburgh, PA, 1606-1615. doi: 10.1061/9780784412848.140
- NZS (Standards New Zealand). 2006. *Concrete structures standard part 1-the design of concrete structures*. NZS 3101:2006, Wellington, New Zealand.
- Paulay, T. & Priestley, M.J.N. 1992. *Seismic design of reinforced concrete and masonry buildings*, Wiley, New York.
- Zhu, S., & Jirsa, J. O. (1983). *A study of bond deterioration in reinforced concrete beam-column joints*. PMFSEL Report No. 83-1, Phil M. Ferguson Structural Engineering Laboratory, University of Texas at Austin, Austin, TX.

ACKNOWLEDGEMENT

This study is supported by the grants from the Ministry of Science and Technology in Taiwan and completed with help of graduate students, Ms. Ying-Ru Lin, Ying-Chieh Chi, and Wei-Ching Huang in the National Yunlin University of Science and Technology. The authors are also grateful to their help and support. A detail list of the test data and database investigation will be published the PhD thesis of Dr. His-Ching Chen in July, 2017.